Numerical analysis of cumulative impact of phytoplankton photoresponses to light variation on carbon assimilation

S. Esposito, V. Botte, D. Iudicone, M. Ribera d'Alcala'

Numerical analysis of cumulative impact of phytoplankton photoresponses to light variation on carbon assimilation

S. Esposito, V. Botte, D. Iudicone, M. Ribera d'Alcala'

PII: S0022-5193(09)00347-6
DOI: doi:10.1016/j.jtbi.2009.07.032
Reference: YJTBI 5652

To appear in: *Journal of Theoretical Biology*

Received date: 4 September 2008
Revised date: 27 July 2009
Accepted date: 27 July 2009

Cite this article as: S. Esposito, V. Botte, D. Iudicone and M. Ribera d'Alcala', Numerical analysis of cumulative impact of phytoplankton photoresponses to light variation on carbon assimilation, *Journal of Theoretical Biology*, doi:10.1016/j.jtbi.2009.07.032

Numerical analysis of cumulative impact of phytoplankton photoresponses to light variation on carbon assimilation

S. Esposito*[a,b], V. Botte[a], D. Iudicone[a], M. Ribera d'Alcala'[a]

[a] *Laboratory of Ecology and Evolution of Plankton, Stazione Zoologica Anton Dohrn, Villa Comunale 1, 80121, Naples, Italy*
[b] *COMORE, INRIA, BP93,06 902 Sophia-Antipolis, Cedex, France*

Abstract

Light variation in temporal and spatial domains is a key constraint on the photosynthetic performance of phytoplankton. The most obvious responses are the modification of cell pigment content either to improve photocapture or to mitigate photo-damage. Very few studies have analyzed whether light variation significantly alters carbon assimilation, especially in a fluctuating light environment as in the mixed layer of the ocean. We addressed the question using a modeling approach, which allows the reproduction of most of the possible scenarios, obtained with great difficulty in laboratory or field experiments. The complete model is based on the dynamic coupling of a photoacclimation and photodamage-repair responses. In this combined model the virtual phytoplankton is exposed to different light regimes (steady, square wave, sinusoidal Light-Dark cycles and fluctuating regimes). The results reconcile controversial results on different photacclimation states achieved during fluctuating light regimes. The model produces a depression of carbon assimilation in any light fluctuating scenario, as compared to steady light regimes, due to the temporal delay between light fluctuations and photoresponses. Those results suggest the possibility of selective pressure during evolution more effective on photoprotective

*Corresponding author
Email addresses: serena@szn.it (S. Esposito), vincenzo.botte@szn.it (V. Botte), iudicone@szn.it (D. Iudicone), maurizio@szn.it (M. Ribera d'Alcala')

mechanisms than on optimization of light harvesting

Key words: phytoplankton, photophysiological models, photoacclimation, photoinhibition, carbon fixation, light fluctuations

1. Introduction

The interplay between mixing and vertical light attenuation on phytoplankton photophysiology and growth rates has been recurrently investigated, however the emerging patterns are often contrasting and a unifying model that reconciles all of the results has yet to be developed. In situ data, and laboratory and numerical experiments show that phytoplankton subjected to fluctuating irradiance connected to mixing may acclimatize to the mean perceived irradiance (Falkowski and Wirick, 1981; Denman and Marra, 1986), or to an irradiance higher (Vincent et al., 1994; Moore et al., 2006) or lower (Behrenfeld et al., 1998; Dusenberry, 2000; Havelková-Doušová et al., 2004) than the mean.

Cullen and Lewis (1988) demonstrated that symmetric transitions between different light intensities induce "hysteresis" in phytoplankton photoresponses, producing acclimation states different from those reached at the mean irradiance. Patterns emerging from non linear responses in a varying light environment are difficult to predict *a priori*. Only a few studies have provided significant insight into the issue.

In 1978 Marra demonstrated the existence of different photosynthetic responses under three regimes (constant light, periodic variation, and fluctuating light). More than a decade later Ibelings et al. (1994) found that the green alga *Scenodesmum protuberans* adapted its chlorophyll content to the maximum light perceived and that the cyanobacterium *Mycrocystis aeruginosa* adapted its photosynthetic pigment content to an irradiance proportional to the average light. Later Havelková-Doušová et al. (2004) used a complex experimental setup and produced a quantitative comparison of the effects produced by fluctuating (i.e., light varying between minimum and maximum in the order of two hours) and non-fluctuating light regimes. Their conclusion was that *Dunaliella tertiolecta*

acclimates to an irradiance lower than the mean irradiance perceived by the cells during a fluctuating regime. Cells exposed to symmetrical variations of irradiance, over a time interval shorter than the time required for the acclimation of the chlorophyll to carbon ratio ($chl\,a : C$) to the new irradiance, tend to achieve values of $chl\,a : C$ closer to the ones induced by lower irradiance. This results in a larger light harvesting capacity as compared to cells grown in non-fluctuating illumination at the same Total Day Light Dose (TDLD). Surprisingly, the cells grown under fluctuating regime displayed growth rates comparable to those grown in stable sinusoidal irradiance, i.e., with no simulated mixing and at higher TDLD. The authors hypothesized that very fast photoprotective mechanisms from high irradiances, e.g., state transitions of photosystems, together with the increased light harvesting were the cause of the good growth performance to a highly dynamic simulated environment. The presence of a double pattern of acclimation: to an irradiance related to the TDLD for the light harvesting, and to an irradiance closer to the peak irradiance for the photoprotection mechanism through state transitions, has been confirmed also in the work by Garcia-Mendoza et al. (2002) on the green alga *Chlorella fusca* .

Similar experiments conducted on diatoms showed a even wider range of responses. The Antarctic diatom *Chaetoceros brevis* acclimatized to the TDLD and was impaired in its growth rate by fluctuating light with 3-hour period, likely because of an increased energy demand for repairing the photosynthetic apparatus in fluctuating light with that frequency (van Leeuwe et al., 2005). *Phaeodactylum tricornutum* increases the photoprotective pool pigments in fluctuating regimes leading to a down-regulation of photosystem II (PSII) by up to 90% and virtually eliminating photoinhibition (Lavaud et al., 2002). The Lavaud et al. (2002) study left open the question of the real impact of that acclimation response on growth, which was not monitored. Wagner et al. (2006) estimated that cultures of the diatom exposed to fluctuating light regime achieved a very high conversion efficiency of photosynthesis, and that almost all the energy feeding the electron transport chain was converted into biomass, and not lost through other electron sinks. By contrast, the green alga *C. vulgaris* seemed

to convert solar energy to biomass formation with a lower efficiency, because energy dissipation through state transitions down-regulated the carbon fixation at fluctuating irradiance. It is clear that some photophysiological responses are highly dynamic and cope well with an intermittent light regime, e.g., state transitions. However, the effective cost of the different physiological states in the conversion of energy into biomass is a crucial aspect of fitness, and it is still poorly known.

In addition, mixing might also mitigate photoinhibition by reducing the time of exposure of cells to high light, thus partially compensating for the decrease of production due to the decrease of irradiance (Kamykowski et al., 1994; Franks and Marra, 1994; Farmer and McNeil, 1999; Nagai et al., 2003; Cianelli et al., 2004).

In synthesis, a wide spectrum of photoresponses have been observed in phytoplankton. Cells tend to maximize light-harvesting at low light, and to mitigate the damage due to irradiance excess in many different ways. Fluctuating irradiance may enhance both those features. However the interplay among maximizing light harvesting and mitigating the risk of photodamage during conversion of energy to biomass is still unclear.

Experimental set-ups of highly dynamic scenarios, which might resemble natural variability, are hard to attain. For this reason many studies have been carried using numerical models. Nevertheless, rigorous estimates of the resulting carbon fixation rates under realistic forcings are limited to descriptions of specific photoresponses, and restricted to few physical scenarios. Cianelli et al. (2004) made the first attempt to combine dynamic photo-acclimatation of the pigment content with a mechanistic description of photoinhibition and its impact on growth. A similar path was later explored by Baklouti et al. (2006a), but the overall impact of the interaction of photoresponses under realistic forcing was not quantified.

Being aware that a comprehensive mechanistic model of all photophysiological responses of phytoplankton is still far from being achievable, we assembled a model which mimics, through simplified mechanisms, the coupling of regulation

of the light harvesting system and responses to excess light. This does not aim to produce a better fit to an observed subset of physiological responses but, in order of importance, to analyze in more detail the effect of that coupling on carbon assimilation, and to formulate hypotheses on the possible advantage for which such responses were selected.

The results discussed here are part of an integrated study including the analysis of the simulated responses in realistic mixed layer dynamics, as reproduced by a Large Eddy Simulation. In this contribution we first describe the assumptions and the parameterization of the photophysiological model and its calibration vs. an experimental data-set. Then we present the acclimation states of phytoplankton exposed to different idealized fluctuating irradiance regimes, in order to analyze their impact on carbon assimilation. Finally we explore the dependence of the model, and thus of the virtual physiology, on the different values in the parameters.

2. The photophysiological model

Our photophysiological model, presented in Table 1, is based on the "GM3" version of the Geider (1998) model as modified by Flynn et al. (2001).

The Geider model describes phytoplankton growth as a function of both environmental variables (external nitrogen concentration and irradiance) and cell chemical composition. The acclimation model has been coupled with the model by Han (2002) in order to include photoinhibition. The coupling is different from recent versions of an acclimation-inhibition model (Cianelli et al., 2004; Baklouti et al., 2006a,b) because both constituting modules (photoacclimation and photoinhibition) are different from Cianelli et al. (2004) and the coupling technique is different from both. Han's model is a dynamical mechanistic model that includes the mechanism of damage and repair of D1 protein in the regulation of the relative concentration of the functional D1; the model assumes the existence of three states for the PSII, active, inactive and damaged or photoinhibited. The model considers that each photon may damage the D1 protein of

Equations	Equation number
$P^C_{ref} = \frac{n^C}{\tau}\ (1-\beta_c)$	(1)
$\alpha^{chl} = {\alpha^{chl}}_{ref}\ (1-\beta_c)$	(2)
$P^C_{max} = P^C_{ref}\ \left(\frac{Q-Q_{min}}{Q_{max}-Q_{min}}\right)$	(3)
$PS = P^C_{max}\left[1-\exp\left(\frac{-\alpha^{chl}\,\theta\,E}{P^C_{max}}\right)\right]$	(4)
$V_N = P^C_{ref}\,Q_{max}\,S\,\frac{1-Q/Q_{max}}{1-Q/Q_{max}+shape}\,\frac{N}{N+K_N}$	(5)
$resp = V_N\,N_{cost}$	(6)
$\rho_{chl} = \theta^N_{max}\,\frac{PS}{\alpha^{chl}\,\theta\,E}$	(7)
$\frac{dQ}{dt} = Q\,V_N - Q\,\frac{1}{C}\,\frac{dC}{dt}$	(8)
$\frac{d\theta}{dt} = \theta\,V_N\,\rho_{chl} - \theta\,\frac{1}{C}\,\frac{dC}{dt}$	(9)
$\frac{dC}{dt} = C\ (PS - resp)$	(10)
$\sigma_{PSII} = a\,\theta^b$	(11)
$\beta_b = \frac{\sigma_{PSII}\,E\,\tau}{1+\sigma_{PSII}\,E\,\tau+k_d/k_r\,\tau\,(\sigma_{PSII}\,E)^2}$	(12)
$\frac{d\beta_c}{dt} = -k_r\,\beta_c + k_d\,\sigma_{PSII}\,E\,\beta_b$	(13)

Table 1: Equations of the photophysiological model.

a closed PSII and that the damage to the protein is proportional only to the absorbed photons, and not to the irradiance *per se*, and that its repair rate is independent of the irradiance. We refer to the probability of a photosynthetic unit (PSU) to be in the open, closed or photoinhibited state as β_a, β_b and β_c respectively. Each photon harvested by the antenna of a closed PSII has a finite probability to damage it. This probability is quantified by a constant k_d. Accordingly the probability that a closed PSU becomes inhibited is given by the product of $k_d\,\sigma_{PSII}\,E$ in Eq. 13 in Table 1, where $\sigma_{PSII}\,E$ is the irradiance absorbed by the PSII (σ_{PSII} being the functional cross section of the PSII and E the irradiance). The number of PSUs in the photoinhibited state increases at high irradiances as the probability of the reaction center of the PSII to be in the radical form increases. The rate of repair of the D1 protein is constant and irradiance independent, and is given by k_r that is expressed in s^{-1}.

The Geider model is based on the assumption that the decrease in pigment content at high irradiance is due to an internal regulation of the biosynthetic process, presumably aimed at decreasing the risk of photoinhibition at high light intensity. Nonetheless, the latter process is not included. The new feature introduced in our model is the compensatory "photoprotective" effect of down-regulation of the pigment content in the coupling between the photoacclimation and photoinhibition parts of the model, which should improve the model capability of mimicking the time course and regulation of photoresponse to variable light. The most prominent mechanisms to decrease the algal pigment content at high irradiance are: 1. a decrease in the total number of reaction centers per cell (n-strategy); 2. a decrease of the pigment content of the PSU antenna (keeping the number of reaction centers constant (σ-strategy) (Falkowski and Owens, 1980; Perry et al., 1981; Dubinsky et al., 1986; Six et al., 2008)). The model by Geider et al. (1998) does not include those mechanisms and we modified the model to explicitly include the σ-strategy, that consists of changes in the antenna size that modifies the functional cross section for the PSII. This change affects the photoinhibition term because antenna size regulates the light harvested by each PSU and, hence, the probability of damage. We chose to

consider that our phytoplankton population follows this strategy because it is able to reproduce the "photoprotective" effect of the down-regulation of pigment content at high irradiance. We considered that change in the σ_{PSII} accompanies an adjustment of the pigment content, and subsequently we modified the Geider model by making the σ_{PSII} follow the change of Chlorophyll content (represented by the $chla : C$ in Eq. 11), which subsequently changes the damage rate of the photosynthetic units. The relation between σ_{PSII} and $chla : C$ in Eq. 11 is not linear, but exponential with an exponent lower than 1, because pigment packaging limits the increase of σ_{PSII} with $chla : C$. The dynamical description of photoinhibition proposed by Han (2002) has been included in the model, as the number of photosynthetically active reaction centers would be reduced by damage to the D1 protein. For this reason, both α^{chl} (the $chla$-specific initial slope of the PE curve) and P^C_{max} (the Carbon-specific maximum rate of photosynthesis) would also decrease as the damage proceeds, thus increasing the number of photoinhibited reaction centers, according to Eqs. 1 and 2 (derived by Sakshaug et al. (1997)). The decrease in the P^C_{ref}, due to the increase in the relative concentration of damaged reaction centers β_c, modifies the photosynthetic capacity. In Eq. 1, n^C is the total number of reaction centers and the expression $(1 - \beta_c)$ is the relative concentration of undamaged reaction centers that participate in the photosynthetic process. Also, α^{chl} decreases at high irradiance, because photoinhibition decreases the relative number of reaction centers participating in photocapture (via the product of ${\alpha^{chl}}_{ref}$ with the expression $(1 - \beta_c)$). In contrast, modifications in the $chla : C$ ratio and σ_{PSII} do not change the ${\alpha^{chl}}_{ref}$, as they modify the organization of the PSUs, but not their efficiency in photocapture normalized to the chlorophyll.

The relative number of damaged reaction centers β_c is then calculated integrating Eqs. 12 and 13. Equation 12 represent the steady-state solution derived in Han (2002) from the equation for the relative concentration of closed reaction centers (i.e., reaction centers that can be photoinhibited if the rate of damage is greater than the rate of repair). In this work, we chose to not solve dynamically the equation for β_b because the integration time step used in the simulations

(180 s) is significantly longer than the time required for a PSU to pass from the open to the closed state and *viceversa* (Ross et al., 2008). For this reason, the number of closed reaction centers β_b is calculated as at the equilibrium with the actual irradiance, using Eq. 12. The values of β_b calculated in this way are then used in Eq. 13, so that the change in relative concentration of D1 damaged reaction centers is accounted for dynamically: σ_{PSII} in this equation changes because of the modification in pigment content (Eq. 11). This constitutes the feedback of down-regulation of the damage at high irradiance.

The other equations solved by the model are the equation for the maximum and the actual photosynthetic rate (Eq. 3 and Eq. 4 respectively), the nitrogen assimilation (Eq. 5), the respiration (Eq. 6), the regulation term of the chlorophyll synthesis (Eq. 7), the N:C and the $chla : C$ ratio (Eq. 8 and Eq. 9 respectively) and the carbon growth rate (Eq. 10) of the Geider model. Those equations are modified, because the parameters that regulate them (α^{chl} and P^C_{ref}), considered constant in the original model, are changed by the processes of photoinhibition by Eqs. 1 and 2. In general, the formulation of the equations, and the theory behind them, are the same, and have already been discussed in the original papers. Our model includes the reproduction of one strategy of photoacclimation between photoresponses already suggested in the works of Baklouti et al. (2006a) and Cianelli et al. (2004). Moreover it differs from the model recently presented by Ross et al. (2008) because it accounts for the interaction between photoacclimation of the pigment content and photoinhibition through modification of the term σ_{PSII}.

3. Calibration of the model

We calibrated the model with the results of the experiments by Cullen and Lewis (1988). They produced a comprehensive data set, providing time scales of transitions, photosynthetic coefficients and biochemical composition for *Thalassiosira pseudonana* acclimated to three irradiances: low (L 20 $\mu mol\ quanta\ m^{-2}\ s^{-1}$), medium (M 100 $\mu mol\ quanta\ m^{-2}\ s^{-1}$) and high (H 2200 $\mu mol\ quanta\ m^{-2}\ s^{-1}$)

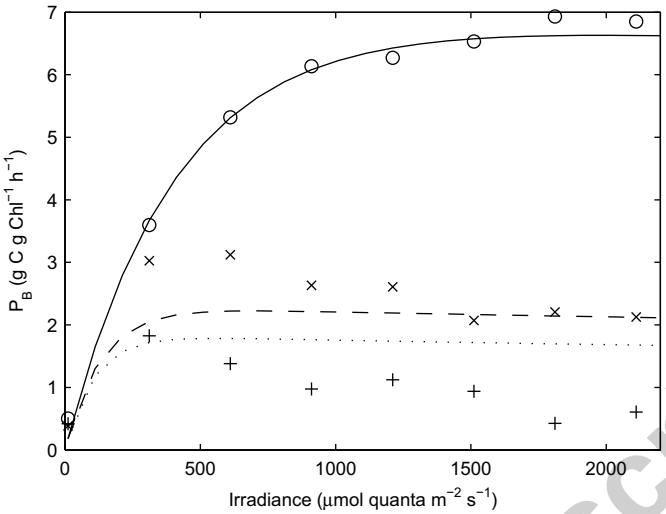

Figure 1: P^BE simulated curves respect to the pseudo-data for *T. pseudonana* grown at three irrandiances. Dotted line and plus signs correspond to LL acclimated, dashed line and crosses correspond to ML, whole continuous line and circles to HL acclimated.

with direct and inverse light shifts among the three. Unfortunately the ^{14}C data were not available. We then generated P^BE curves from the available photosynthetic coefficients with the Platt et al. (1980) equation for Irradiance dependency of production in presence of photoinhibition, and derived pseudo-data from them by adding a random noise to 8 points of the P^BE curves. We then retrieved the parameter values (Table 2) through a least squares fit of the "experimental" pseudo-data and the corresponding model outputs using a constrained non-linear minimization algorithm. We minimized both the distance between the P^BE curves simulated with the model and the P^BE pseudo-data and the distance between the simulated $C : chla$ variations due to the HL-LH, HM-MH transitions and the real data, in order to better reproduce the timescales of photoresponses and the carbon fixation rates.

The model produces P^BE curves similar to the data (Fig. 1) ($R^2 = 0.66$). However it fits better the HL ($R^2 = 0.97$) than ML and LL curves. The damage rates that would have generated LL curves closer to the "experimental" pseudo-data were unrealistically high (to the best of our knowledge). Therefore, we

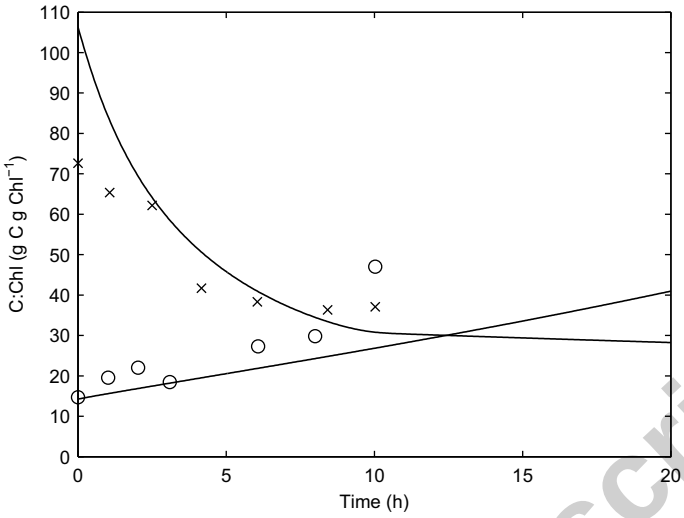

Figure 2: Simulated time course of the $C : chla$ during the shift from HL to LL and LL to HL superimposed on the *T. pseudonana* data. Open circles correspond to the data for the increasing shift while crosses correspond to the data for the decreasing shift.

then decided to keep the parameters values within the limits reported in the literature, except for the repair rate that is slightly larger. The HL acclimated virtual phytoplankton did not show any photoinhibition, which in the model is strongly reduced by the decrease of σ_{PSII} concurrent with the decrease of $chla$ content. By contrast ML and LL curves displayed photoinhibition with lower values of P^B. We suppose that the distance between the LL data and LL simulated curves results from an underestimation of σ_{PSII} at the lowest irradiance connected to the lack of true short term photoprotective mechanisms in the model.

On the other hand an important feature is well reproduced by the model, the '*hysteresis*'. The increase of the $C : chla$ ratio with increasing light proceeds with a slower velocity than its decrease during the opposite shift in irradiance (Figs. 2 and 3).

The time scales reported in Table 3 show that the change in $C : chla$ with irradiance spans from several hours to few days. In addition, more time is required to adjust to a large increase of irradiance compared with a smaller increase. At

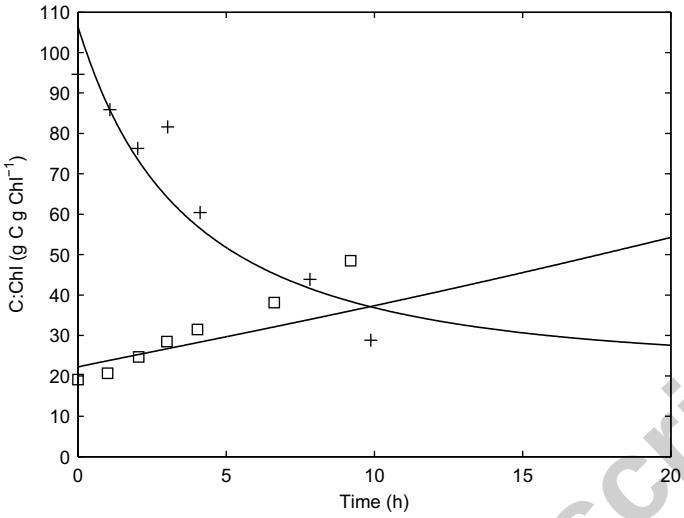

Figure 3: Simulated time course of the $C : chla$ during the shift from HL to ML and ML to HL superimposed on the *T. pseudonana* data. Open squares correspond to the data for the increasing shift while plus signs correspond to the data for the decreasing shift.

lower intensity (LM and ML shifts), in contrast, the pattern is the opposite: acclimation to increasing irradiance is quicker than to a decreasing shift. This is due to the peculiar interplay between carbon fixation and chlorophyll synthesis at very low irradiance as a result of unbalanced growth. Time scales of photoinhibition are shorter, generally less than an hour (Table 3). Photoinhibition also shows a slight hysteresis. The damaging reaction during an irradiance increase is faster than repair during an irradiance decrease. However, slower changes in the functional cross section produce additional indirect changes in the number of damaged reaction centers, as the rate of damage is connected to the functional cross section and consequently to the $chla : C$ ratio. The asymmetry in the kinetics is reproduced during all irradiance shifts and in both directions (see Table 3) as well as the time-scales of the physiological adjustments and the carbon assimilation rates.

Constant (units)	Value	Definition	Range
n_C (g C g C^{-1})	4.48e^{-8}	total number of reaction centers	3.90e^{-9}- 4.43e^{-7}(*)
$\alpha^{chl}{}_{ref}$ (g C g $chla^{-1}$ h^{-1} µmol quanta^{-1} m^2 s)	0.017	linear slope of the P^BE curve without photoinhibition	0.014-0.055(*)
τ (ms)	1.6	turnover time of the electron transport chain	1.2-10.0(*)
k_d (d.l.)	2.8e^{-8}	damage constant	5.3e^{-9}- 2.7e^{-7}(*)
k_r (s^{-1})	1.2e^{-3}	repair rate	0.7e^{-4}- 2.0e^{-4}(*)
θ^N_{max} (g N g $chla^{-1}$)	0.36	maximum *chla* to Nitrogen ratio	0.14-0.39(*)
a (m^2 g C µmol quanta^{-1} g $chla^{-1}$)	15.17	linear slope of the σ_{PSII} to $chla:C$ parameterization	10-50(+)
b (d.l.)	0.4	pigment packaging parameter	< 1(+)
Q_{min} (g N g C^{-1})	0.050	minimum Nitrogen to Carbon ratio	0.039-0.059(x)
Q_{max} (g N g C^{-1})	0.20	maximum Nitrogen to Carbon ratio	0.16-0.18(x)
K_N (mg N L^{-1})	0.1	half saturation constant	0.1-1.3(x)
N_{cost} (d.l.)	3.21	respiration cost for nitrogen assimilation	2.00-3.21(x)
S (d.l.)	0.236 (x)	Scalar for controlling the maximum level of N asimilation	
shape (d.l.)	0.01 (x)	shape factor for control of N assimilation	

Table 2: Parameters for the photophysiological model, their meaning and their ranges of existence in literature.(*) taken by MacIntyre et al. (2002); (+) derived by Baklouti et al. (2006b) and MacIntyre et al. (2002);(x) taken by Flynn et al. (2001)

Variable	SHIFT	this work (h)	logistic model (h)
$T_{50}\ C:chla$	HL	2.91	4.71
”	LH	24.42	12.87
”	HM	3.05	4.04
”	MH	20.35	9.45
”	ML	22.35	14.12
”	LM	8.80	6.98
$T_{\infty}\ \beta_c$	HL	0.70	*
”	LH	0.61	*
”	HM	0.70	*
”	MH	0.63	*
”	ML	0.70	*
”	LM	0.58	*

Table 3: Time scales of 50% acclimations as the time necessary to reach the 50% of the fully acclimated state as derived by the simulations of this work and by the logistic formulation as given by Cullen and Lewis (1988). * photoinhibition was not analyzed by Cullen and Lewis (1988)

4. Performance of the model

4.1. The scenarios

We simulated various scenarios, all including the diurnal variation of illumination and its interaction with light variations produced by simple circular trajectories of the cells in the vertical dimension. All the simulations lasted for at least 7 days. The model scenarios have been taken from Havelková-Doušová et al. (2004) to reproduce their experimental setup.

In order to obtain a reference for model performance at constant irradiance, a first set of simulations were carried out at 220 different irradiances with alternating 12 hours of constant illumination and 12 hours of dark, as distinct from Havelková-Doušová et al. (2004), who set their reference at continuous light regime. This reference, from now on "LD", was chosen to mimic the illumination regimes usually used in laboratory experiments. We performed also a second set of simulations with the 12 hour day light period following a sinusoidal profile typical of diurnal variation. We ran a reference set of simulations for 220 different amplitudes of the sinusoids, mimicking the daily variations of light field at various depths. The values of physiological variables or rates obtained in fluctuating light fields were then compared with those obtained in the two reference scenarios (LD and sinusoidal), plotting them vs TDLD. All the observed differences were due to the variations produced by the circular trajectories versus "calm water" regimes.

The light fluctuations followed these equations (Havelková-Doušová et al., 2004):

$$I = \begin{cases} I_{max}\ \sin\left(\frac{t\,\pi}{D}\right)\ e^{x} & 2k \leq \frac{t}{D} < 2k+1 \quad k = 0, 1, \ldots 9 \\ 0 & 2k+1 \leq \frac{t}{D} < 2k \quad k = 0, 1, \ldots 9 \end{cases} \tag{14}$$

$$x = -k\,h\,\frac{\sin\left(\frac{2\,\pi\,t}{P} + \frac{\pi\,t_0}{D}\right) + 1}{2} \tag{15}$$

where I_{max} represents the maximal irradiance at noon (here 970 μmol *quanta* m^{-2} s^{-1}), D the photoperiod (here 12 h), k the diffuse attenuation

coefficient. We explored 5 values of k representing Jerlov's oceanic water types IA, IB, II and III, and one coastal water type. However, for clarity, we show results only for IA and coastal waters. P and h represent respectively the complete rotation period and diameter of the cell trajectories, i.e., the depth of the hypothetical mixed layer. $P = h * 2/vel$ with vel being the typical circulation velocity of moving cells derived from simulations with the Large Eddy Simulation (Esposito et al, unpublished data). It is worth noting that the diurnal sinusoidal signal and the circulation of the phytoplankton overlap thus generating many more regimes. The time when "phytoplankton reach the surface" (t_0) can generate covariance with the diurnal modification as well as antivariance. t_0 is considered to vary between 1 and 24, the hour corresponding to the first time that the phytoplankton are at the surface. The simulations explored a wide range of TDLD with different values for k, P, t_0 and h corresponding to typical idealized timing and velocities in mixed layers of different depth and turbidity (summarized in Table 4).

We chose to study the model performance when full acclimation to the specific irradiance regime was reached. The results presented here concern the mean photophysiological properties and the mean carbon growth rates found in the last day of simulation. We performed averages between the different simulations that differ only for the hour when phytoplankton reached the surface.

4.2. Chlorophyll to Carbon ratio

The mean $chla : C$ of the last 24 hours of simulations at LD cycle as a function of TDLD decreases from 0.08 g $chla$ g C^{-1} at the lowest TDLD (~ 1 mol quanta m^{-2}) to 0.04 g $chla$ g C^{-1} at the highest TDLD simulated (~ 40 mol quanta m^{-2}, Fig. 4). The sinusoidal irradiance produces similar mean values although the diurnal acclimation was different (data not shown). Simulations with fluctuating regimes in clear waters at highest TDLD (very shallow MLD) show mean $chla : C$ ratios similar to the values of $chla : C$ simulated at constant or "calm water" light regimes with comparable TDLD (white symbols in Fig. 4). However at deeper MLD the $chla : C$ ratios are greater than the corresponding

k (m^{-1})	Range of h (m)	vel ($cm\,s^{-1}$)	symbols
0.037	10-100	0.1	open squares
0.053	10-100	0.1	
0.085	10-100	0.1	
0.1275	10-100	0.1	
0.3	10-100	0.1	filled squares
0.037	10-100	0.5	open circles
0.053	10-100	0.5	
0.085	10-100	0.5	
0.1275	10-100	0.5	
0.3	10-100	0.5	filled circles
0.037	10-100	1	open triangles
0.053	10-100	1	
0.085	10-100	1	
0.1275	10-100	1	
0.3	10-100	1	filled triangles

Table 4: Water turbidity as the estintion coeffitient, spatial scales as the depth of the mixed layer and velocities of circulation in the mixed layer in the simulations with fluctuating irradiances and the symbols associated in the figures.

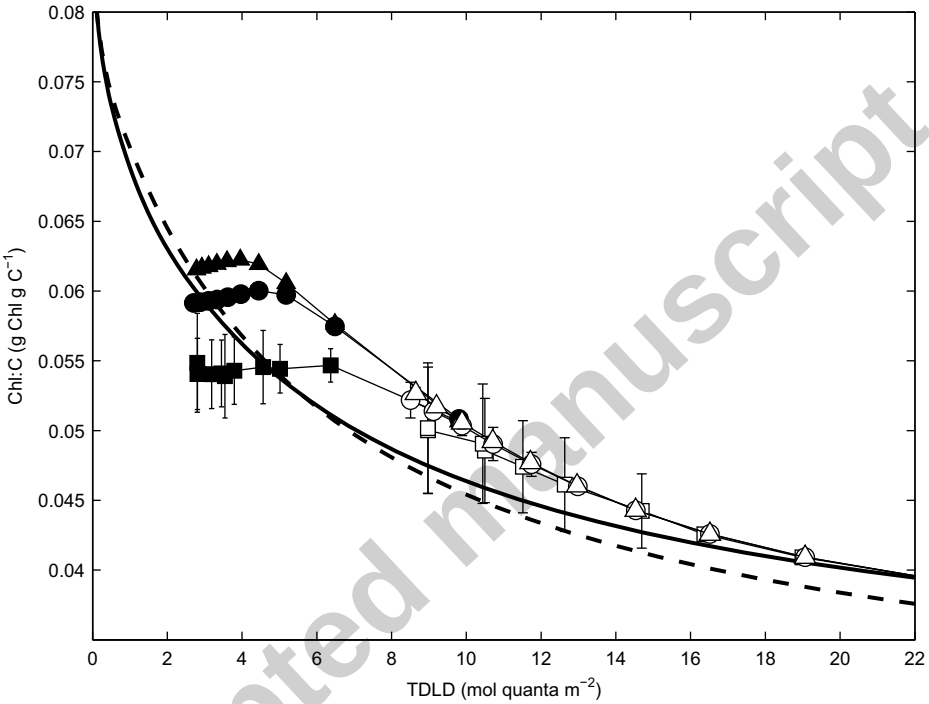

Figure 4: Daily mean $chla : C$ as a function of the TDLD at different Irradiance intensities and frequencies of the fluctuations: dashed line corresponds to the LD simulations, continuous line to the sinusoidal irradiances, while the black filled symbols represents the different velocities in the range of MLDs explored for Coastal waters and the black open symbols the velocities associated to mixing in Oceanic water type IA. Error bars correspond to the standard deviations between simulations that differ from the hour when phytoplankton reach the surface. Squares correspond to the slowest circulation velocities, circles to the intermediate and triangles to the quickest velocities. Details are given in Table 4

values in calm waters. For coastal waters (black symbols) a double pattern emerges. For fluctuations in deep, turbid layers mixed at low velocities (black squares and circles at low TDLD in the figure) the $chl\,a : C$ ratios are lower than the values found for simulations in calm waters. Then phytoplankton acclimate as if is experiencing higher stable irradiances. The pattern reverses in the other turbid cases where phytoplankton acclimation is typical of lower stable irradiances and resembles the clear water cases. It is remarkable that these mean values mask a huge difference between simulations with different t_0 (data not shown), because the hour when phytoplankton reach the surface during the last day strongly influences the ratios.

The former result is different from that reported by Havelková-Doušová et al. (2004). In that study, phytoplankton under fluctuating light always showed a $chl\,a : C$ ratio higher than the $chl\,a : C$ ratio found in the square-wave and sinusoidal regimes. It is worth noting that Havelková-Doušová et al. (2004) laboratory experiments were performed using an extinction coefficient for light twice as large as the highest used in our scenarios, within a virtual, very shallow, intensely mixed layer of 5 m. Phytoplankton grown under those fluctuating irradiances show a $chl\,a : C$ ratio typical of a lower non fluctuating TDLD.

In our simulations this pattern holds for several regimes: for high velocity fluctuations, for intermediate mixed layer depths and high turbidity, and for a deep clear mixed layer. The light variations corresponding to the clear and shallow MLD are so slow that phytoplankton have time to fully acclimate to the changing irradiance, and there is no significant hysteresis. By contrast, in very turbid deep mixed layers, the time scales of adaptation to light shifts at low intensity (ML and LM shifts in Table 3) are such that acclimation to increasing irradiance proceeds more quickly than acclimation to the opposite decreasing shift, thus shifting the acclimation toward a high light adapted state. Dusenberry (2000) suggested that differential rates of photoacclimation to upward or downward shifts in irradiance might enable phytoplankton to grow better in a turbulent environment. The increase in light-harvesting efficiency, reported by Dusenberry (2000), is matched in many of our scenarios, but another term is

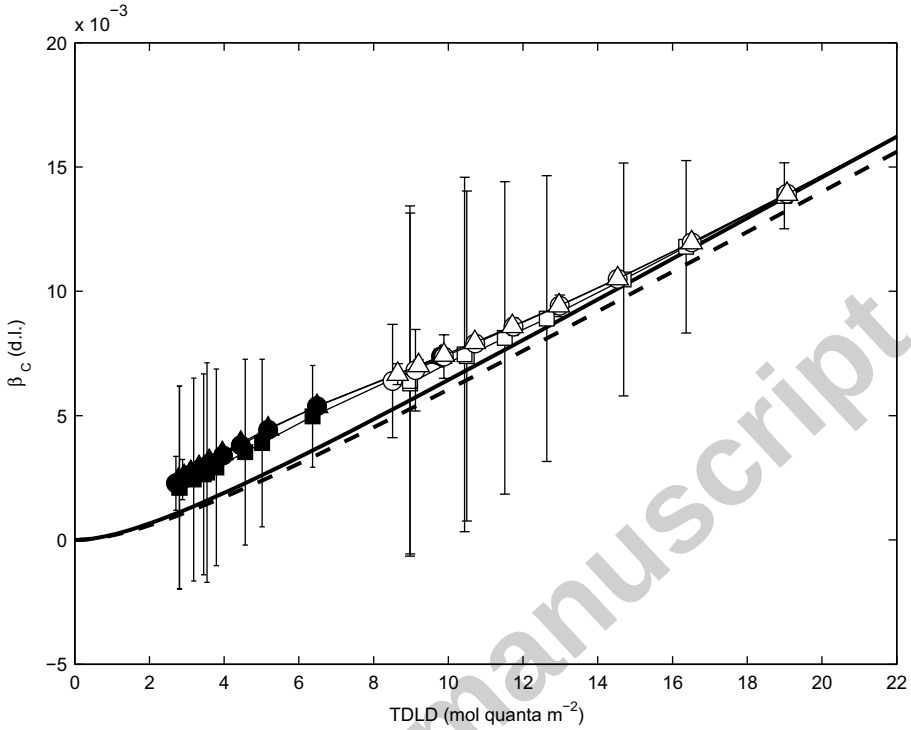

Figure 5: Daily mean relative number of photoinhibited reaction centers as a function of the TDLD at different Irradiance intensities and frequencies of the fluctuations. Symbols as in Fig. 4

important to determine carbon fixation rates.

4.3. Photoinhibition

Photoinhibition increases with the TDLD in LD as well as in sinusoidal irradiance (Fig. 5), reaching a daily average of 4 % of damaged reaction centers at the highest TDLD (data not shown). Sinusoidal irradiance produces a similar pattern with a slightly higher inhibition due to the higher irradiance reached at the apex of sinusoidal curve for the same TDLD. Those results mask great variation between simulations that belong to the same physical scenarios but differ in the timing of cell displacements. Cells that gain advantage from this timing show near zero inhibition, whereas other cells can be strongly photoinhibited

by the same physical scenarios. However on average, photoinhibition in mixed water is greater than that in calm water, and phytoplankton exposed to rapid fluctuations is more photoinhibited than that exposed to slow ones. Actually, in clear and shallower mixed layers (high TDLD white symbols), photoinhibition is comparable to that found under non-mixing regimes.

Also photoinhibition displays hysteresis. The repair is always slower than the damage for the same symmetrical shift of irradiance (as already evident in Table 3). As a consequence, in the model, the damage due to fluctuating irradiance is always greater than the damage produced by a light dose supplied with LD or sinusoidal pattern.

Our comparisons are for equal TDLD's. Therefore, higher photoinhibition observed under fluctuating irradiance does not indicate that phytoplankton in intensely mixed water are more damaged than in stable water columns. Because the damage is dose-dependent, a lower TDLD, which corresponds to cells escaping the upper inhibiting irradiance especially in a turbid environment, mitigates photoinhibition. In fact, surface mean daily photoinhibition under clear sky reaches 1.5% of damaged reaction centers in calm water condition (the photoinhibition connected to sinusoidal irradiance with the highest TDLD) and less than 0.5% in rapidly and deeply mixed conditions (the photoinhibition of the fluctuating regimes with the lowest TDLD). In brief, for the same TDLD, light fluctuations enhance photoinhibition. In contrast, photoinhibition decreases in a fluctuating regime because of the decrease of TDLD, which will also have a negative effect on the total productivity of the mixed layer.

4.4. Carbon fixation rates

Many studies (Dusenberry, 2000; Franks and Marra, 1994; Nagai et al., 2003) suggest that the interaction of photoacclimation and mixing increases the integrated primary production in the water column. One reason is the above mentioned relief from photoinhibition due to mixing (Franks and Marra, 1994; Nagai et al., 2003). The second reason is the increase of productivity due to the change of the $chla : C$ ratio in the upper mixed layer (Dusenberry, 2000).

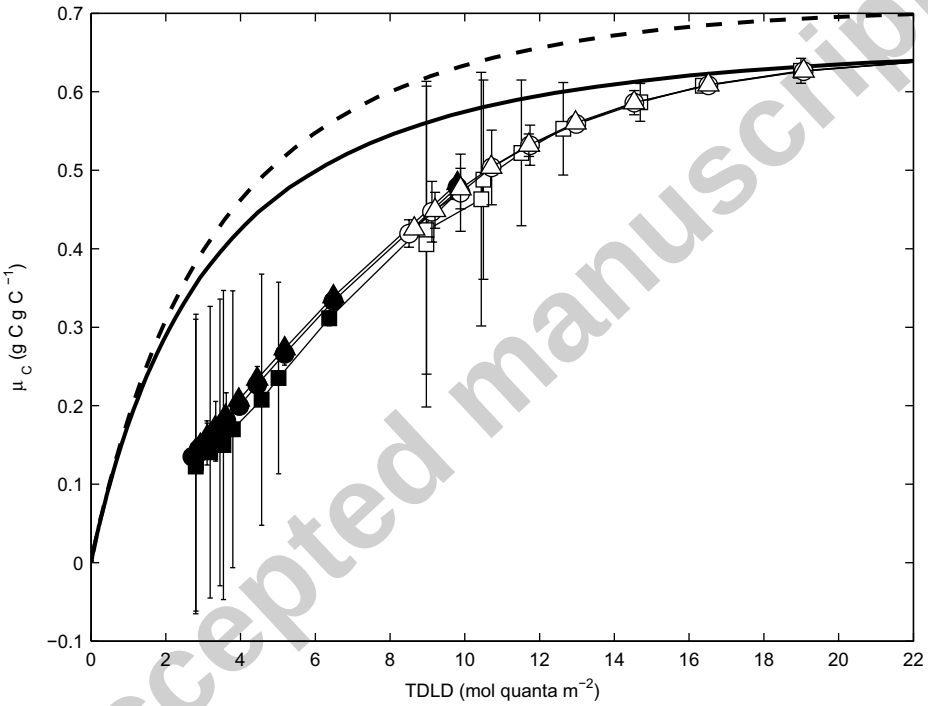

Figure 6: Daily mean carbon growth rates as a function of the TDLD at different Irradiance intensities and frequencies of the fluctuations. Symbols as in Fig. 4.

In our simulations, the mean carbon fixation rate at square wave irradiances is 0 for irradiance very close to 0 and 0.78 d^{-1} at the highest TDLD (Fig. 6). The corresponding maximum values at sinusoidal irradiance is 0.65 d^{-1} at highest TDLD ($\sim$ 25 mol quanta m^{-2}). The presence of the sinusoidal diurnal signal produces carbon fixation rates lower by approximately 10% at higher TDLD. The difference between stable and fluctuating light regimes is even larger, with the stable light fixation rates being always higher. The stable light carbon fixation rates are more than two times larger than the fixation rates in a fluctuating regime. This corresponds to a fixation rate of more than 0.3 d^{-1} for the first and more than 0.1 d^{-1} for the fluctuating irradiances with TDLD of approximately 3 mol quanta m^{-2}. The difference between fluctuating and non fluctuating regimes decreases at the highest TDLD (clearer and more stable virtual water column). Simulation with high TDLD sinusoidal irradiances and fluctuating regimes produces comparable carbon assimilation rates, as well as photoacclimation parameters $chla : C$ and β_c.

In our model, photoacclimation produces the highest growth rates if the phytoplankton is fully adapted to the growth irradiance, and each perturbation of irradiance decreases the averaged daily carbon assimilation. At intermediate mean fluctuating irradiance, the increased light harvesting ability, reflected by higher $chla : C$ s not sufficient to provide an advantage to phytoplankton. It is evident averaging simulations that differ in the interplay between slow displacements and diurnal signals masks high variability of carbon fixation rates. Comparing the mean carbon rates, the difference between physical scenarios is less important than the difference due to the timing of cell displacements, at least in the turbid scenarios. However on average, the continuous mismatch between irradiance perceived and instantaneous photobiological state, decreases the net growth rates of virtual phytoplankton, even if for some, individual cell trajectories, mismatch can increase carbon fixation.

Havelková-Doušová et al. (2004) compared only sinusoidal and fluctuating experimental growth rates. Their experimental results show that cells grown under a sinusoidal regime with superimposed fluctuations have growth rates

comparable with those under the highest total dose of photons supplied with simple sinusoidal illumination. Our results suggest that the growth rate difference between sinusoidal and fluctuating illumination depends heavily on the choice of fluctuating scenario.

4.5. The influence of the non-linearity of the PE curve

From the previous analysis, we conclude that non-linear interactions between photophysiology and light fluctuations cause mean assimilation rates to be lower than those under steady light regimes. However, there are at least two non-linear terms in phytoplankton photobiology. One already discussed and linked to photoacclimation and photoinhibition, and the other embedded in the non-linear shape of the $P^C E$ curve. Efficiency in carbon fixation is higher in the linear part of the curve than at light saturated irradiances.

In order to find out the pure impact of photophysiological adjustments on the resulting carbon fixation rates, we calculated the carbon fixation rates of individuals subjected to the identical light history of the previous simulations, without any dynamical photoacclimative response. In other words the rates for each light intensity are derived from the $P^C E$ curve correspondent to the LL $P^{chl} E$ curve in Fig. 1. Therefore any detected change in the carbon fixation rate depended only on the non-linear shape of the $P^C E$ curve. In addition, no triggering of hysteresis is included. This approach can help to discriminate and quantify the real impact of the photophysiological adjustments on carbon fixation by virtual phytoplankton. Figure 7 shows that carbon fixation rates during LD static simulation at the highest TDLD are almost three times higher than those during dynamic adaptation. At low photon supply rates, the dynamic simulations perform better. The dynamic acclimation impairs phytoplankton exposed to high TDLD, but favours phytoplankton subjected to low TDLD, especially if subjected to fluctuating irradiance. The advantage of dynamical acclimation is evident at low and fluctuating TDLD because pigment content increases at low light favours photocapture by phytoplankton.

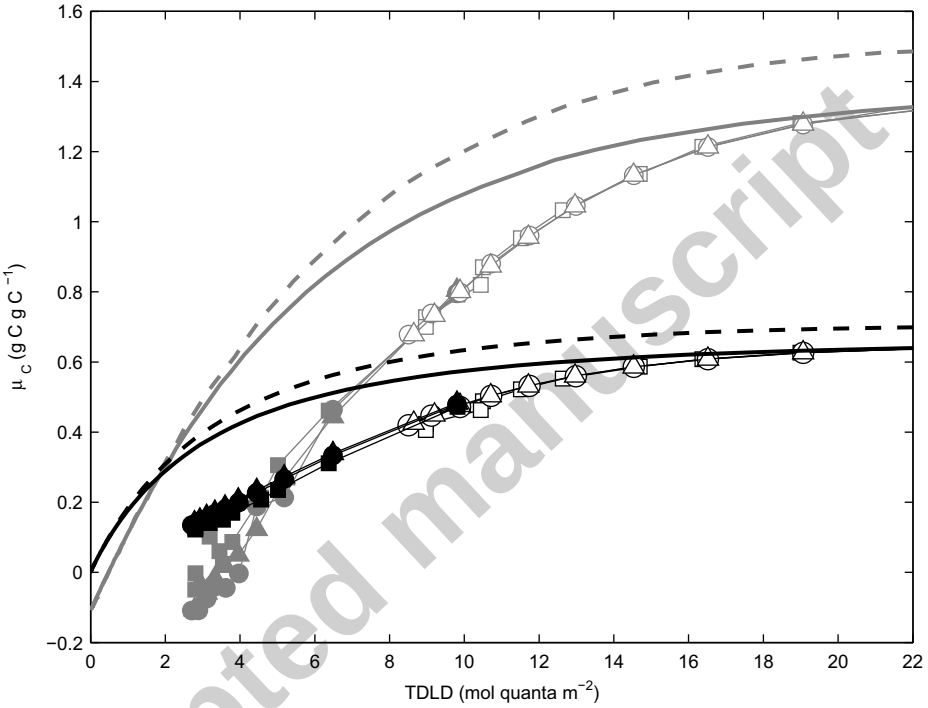

Figure 7: Daily mean carbon growth rates as a function of the TDLD at different Irradiance intensities and frequencies of the fluctuations as in Fig. 6, with superimposed in grey the homologous of the results for the 20 $\mu mol\ quanta\ m^{-2}\ s^{-1}$acclimated mean static carbon growth rates. In detail, grey dashed line corresponds to the LD static simulations, grey continuous line to the static simulation for sinusoidal irradiances. Filled grey symbols correspond to coastal waters and open grey symbols to the type IA waters results for the static carbon growth rates. Squares correspond to the slowest circulation velocities, circles to the intermediate and triangles to the quickest velocities. Details are given in Table 4

4.6. The impact of σ_{PSII}

In the model, the drawback of dynamic acclimation at high TDLD is likely to increase because the large light-harvesting capacity due to the intermittent regime implies an increase in the optical cross section of the photosystems. This in turn amplifies photoinhibition without sufficiently compensating with an increase in photocapture, as photosynthesis is frequently saturated at high TDLD. However, we explored the results derived by simulations with a constant σ_{PSII}, to clarify whether the increased cross section of the PSII produces higher inhibition under fluctuating irradiances.

The results show that fluctuating irradiance produces increased photoinhibition even without considering the effect of increased cross section of the PSII (Fig. 8). This in turn shows that those results do not derive only from the mechanistic link between σ_{PSII}, photoinhibition and photoacclimation we introduced in the model, but also from the intrinsic hysteresis of the photoinhibition.

4.7. Sensitivity analysis

Finally, we performed a sensitivity analysis to quantify the dependence of model results on different parameters. We explored the range of values reported in the literature for each parameter. We performed simulations changing one parameter at a time for three sets of simulations with the minimum, the medium and the maximum value for each parameter. The ranges are reported in Table 2.

The diagnostic variable was carbon assimilation rate. Figure 9 shows carbon fixation rates of the reference simulation. The reference results derive from the simulations discussed above, with parameters taken from calibration of the experiments with *T. pseudonana*. Figure 10 shows the ratio between the carbon fixation rates derived by the parameters varying as indicated, and the corresponding reference simulation.

Variations in the parameter values may depend either on uncertainty in laboratory measurements or on phylogenetic traits. Figure 10 shows that all variations produce monotonic changes in the carbon fixation rates. For example, increasing the turnover time of the electron transport chain τ decreases the

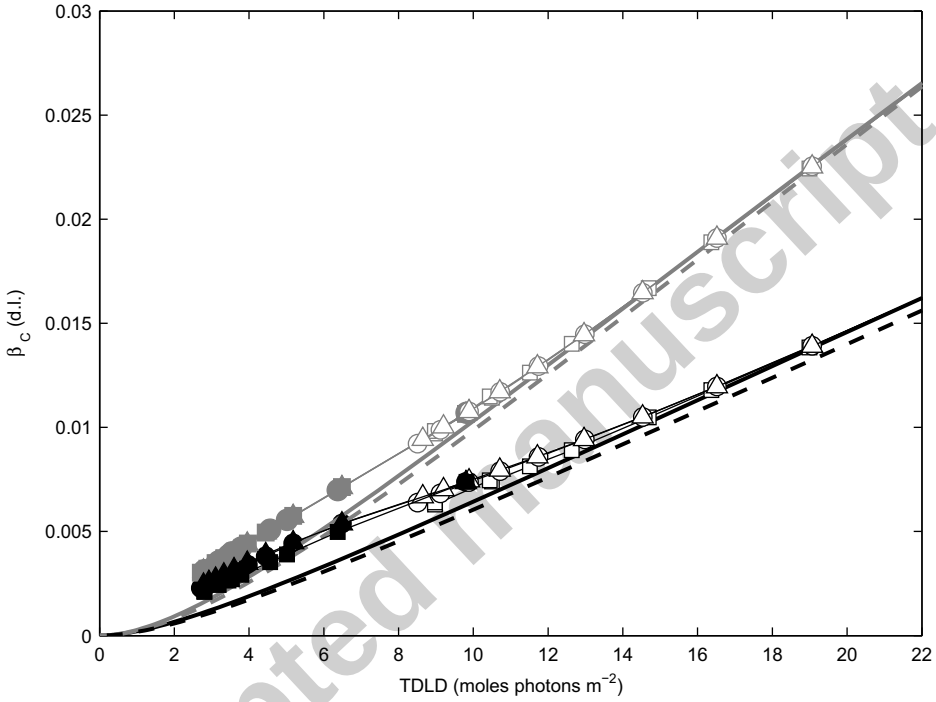

Figure 8: Daily mean relative number of photoinhibited reaction centers as a function of the TDLD at different Irradiance intensities and frequencies of the fluctuations as in Fig. 5 with superimposed in grey the results for the simulations with constant $\sigma PSII$. In detail, grey dashed line corresponds to the LD simulations, grey continuous line to thesimulation for sinusoidal irradiances with constant $\sigma PSII$, filled grey symbols correspond to coastal waters and open grey symbols to the type IA waters results with constant $\sigma PSII$. Squares correspond to the slowest circulation velocities, circles to the intermediate and triangles to the quickest velocities. Details are given in Table 4

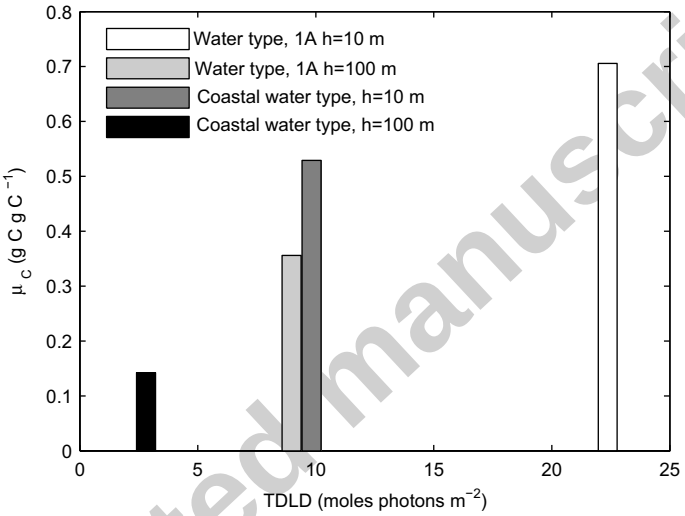

Figure 9: The mean Carbon growth rates of four selected sets of simulations of the reference simulations as a function of the mean TDLD. The colors of the bars are associated to the simulations as indicated by the legend. White and grey correspond to the sets of simulations with clear water and a mixed layer respectively 10 and 100 meters deep, while dark grey and black to a turbid water with a mixed layer respectively 10 and 100 meters deep.

carbon growth rates in all scenarios. The other parameter with a strong influence on fixation rates is the total number of reaction centers, n_C. Variations of n_C value mostly affect the results for the more stable case explored. In our model, the maximum carbon fixation rate is the ratio between n_C and τ and therefore the n_C value directly influences the resulting fixation. Also, an increase of ${\alpha^{chl}}_{ref}$ up to the maximum value of α^{chl} found in literature increases the resulting fixation rate by 50 %, and is most effective at low TDLD's.

5. Discussion and Conclusions

We present a model which reproduces a crucial feature in photophysiology: the time scales of phytoplankton photoresponses, i.e. the change in $chl\,a : C$ and the decrease of photosynthetic performance due to photoinhibition. The mechanisms described by the model are strongly simplified compared with the wider range of mechanisms occurring in real phytoplankton; these mechanisms do not model the xanthophyll cycle, state transitions, etc., nor other crucial mechanisms related to carbon fixation, such as biochemical regulation of the turnover time. However, because the model was calibrated with real kinetics, and photacclimation data fit them satisfactorily, we conclude that it captures important patterns of phytoplankton responses to light variations, in particular the rate of change of photosynthetic performance due to tuning of the light harvesting apparatus and the presence of photoinhibition. Our intent was to analyze the implications of simulated photoresponses on phytoplankton growth, whose only proxy in our approach is carbon assimilation. We explored most of the possible light variation modes, and the impact of different parameters on the response. This was because many experiments were necessarily carried out in simplified scenarios and generally highlighted steady state conditions. The first interesting result of the simulations is that the illumination regime (sinusoidal or square wave) affects carbon assimilation rate. This is an emergent pattern deriving from nonlinear interactions among light variation and photoacclimation, and is not due to the hyperbolic shape of the $P^B E$ curve. We interpret this

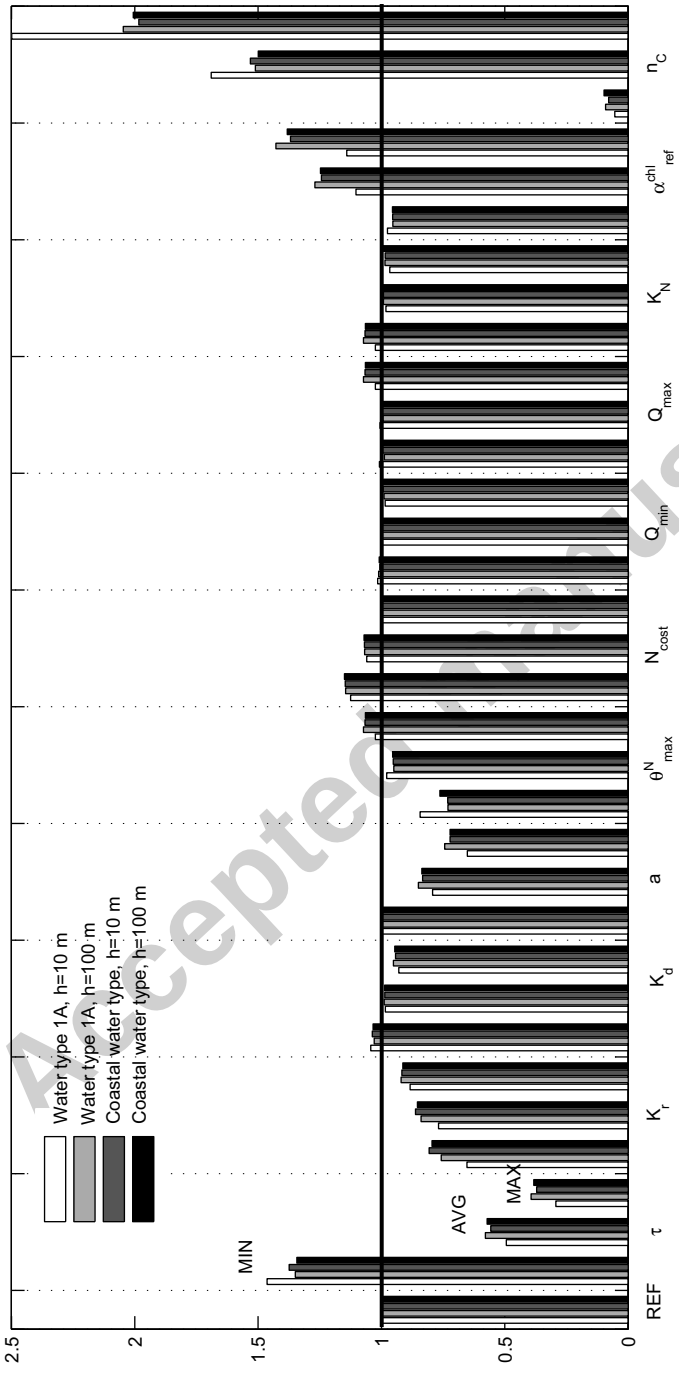

Figure 10: Sensitivity analysis for one-at-the time modification of each parameter of the model. On the Y-axis is reported the ratio between the averages of the Carbon growth rates of the selected sets of simulations and the reference simulations. On the X-Axis the modified parameter. For each parameter on the X-axis the first four bar corresponds to the ratios obtained with the minimum values of the range of existence of the parameter indicated, the second one to the mean value and the third one to the maximum. The colors of the bars are associated to the simulations as in Fig. 9 and indicated by the legend.

as due to the mismatch between the physiological state at a certain time and the light field at the same time. Apparently the sinusoidal light regime always keeps photosynthetic organisms far from their optimal photoacclimation state, which is what is found in typical experimental setups. We believe that this pattern is amplified by the simplifying assumptions of our model, which neglects any circadian regulation of photophysiology. In fact, studies on daily rhythms (e.g., Anning et al., 2000; Ragni and Ribera d'Alcala', 2007, and references therein) suggest that the circadian light variation does not produce the same photoacclimation response observed in light transitions. This, in turn, suggests that more complex regulations are in play. On the other hand, our simulations reconcile some of the contrasting results reported in the literature. We found an increase in light harvesting capacity in phytoplankton displaced in deep and well mixed water columns, as anticipated by Cullen and Lewis (1988) and Havelková-Doušová et al. (2004). In addition, our results suggest that phytoplankton in mixed coastal waters show a state typical of phytoplankton acclimated to higher irradiance. Vincent et al. (1994) observed similar response in a turbid estuary and Moore et al. (2006) reached the same conclusion from fluorescence-based measurements conducted on the shelf. It is therefore remarkable that the model can mimic the high variability of acclimation states and reconcile contrasting evidence found in nature.

At high light regime, the induced decrease of photocapure produces a net loss even if it mitigates photoinhibition. This might results from the lack of explicit photoprotective mechanisms,e.g., xantophyll cycle, in the model. However, the simulated photoinhibition matches quite well the time scales and the amplitude observed in real organisms. We then assume that our model embeds the effects of photoprotection, even without directly modeling it. As a matter of fact, the recovery constant k_r is larger than the values reported in the literature, which compensates for the lack of any photoprotective mechanism in the model.

We assumed that the entire population behaved in exactly the same way; in other words, we represented the response of a non diffusive patch. It is worth noting the great variability of the carbon fixation rates between simulations that

belong to the same physical scenario but differ for light varying in the same or the opposite direction of the diurnal cycle. Here we discussed only the properties averaged over all the phase shifts. If variations occurs at low rates, the importance of these phase and sign shifts is surprisingly high. Since those differences are significant, a greater attention should be paid in formulating photosyntetic adaptation to circadian light variability in models. These simulations represent a small number of simplified light histories of phytoplankton. This aspect will be clarified by a parallel analysis of the results of an Individual Based Model, in which thousands of virtual phytoplankon cells have been displaced in the water column using trajectories derived from a Large Eddy Simulation. We conclude that, even with the inclusion of photoinhibition, these results support the idea of Raven (1980) , that photoacclimation is not to optimize growth but to minimize risk, i.e., reduces mortality rather than increases growth. This in turn suggests that mixing, which generates light variability, should have selected more for protection than that to improve photocapture. This does not seem obvious since the light environment phytoplankton occupy is seldom at high intensity, which should make the risk of irreversible damage infrequent. Pursuing that line of thought, we would then expect that it would be profitable to possess specialized pigments to improve photocapture in specific spectral regimes (Huisman et al., 2004, e.g.,) , or to tune photocapture more efficiently in very stable environments (permanently stratified systems), and especially at depth, where photocapture is the dominant term governing photosynthesic rates.

We cannot distinguish between carbon assimilation, which is the biomass increase, and division rate, which, besides the regulation of the cell cycle, is connected with the use made of carbon. In addition, in our simulations, nitrogen was never limiting but had to be included because of the link between uptake and light.

The photophysiological traits of different species of phytoplankton have an important influence on the model. We show that ontogenetic photoacclimation, even exploring a wide part of parameter space, on average reduces carbon assimilation. However, the sensitivity analysis is based on a hypothetical "species",

which exhibits an ideal coupling of physiological parameters which do not necessarily exist in any living species. The sensitivity analysis highlights that crucial terms in carbon assimilation are the turnover time of the photosynthetic unit, the number of photosynthetic units at high light, and the photoharvesting capacity at low light which is what implicit in a P^BE curve. Besides that, the sensitivity tests also show that the possible advantages/disadvantages vary monotonically with rates of light variation. Although our model reproduces only ontogenic variations due to photoacclimation of the pigment content and photoinhibition, it is known that at increasing irradiance decreased turnover time of the electron transport chain through induction of Rubisco activity is possible (MacIntyre et al., 1997). From this study, we conclude that the resulting effect will cope with increased carbon fixation, mostly in stable scenarios. It is noticeable however that MacIntyre and Geider (1996) showed that timescales of Rubisco induction can rapidly generate positive non-linear effects in turbid and turbulent environments. Our model lacks this possible positive effect on carbon fixation. An alternative strategy proposed for acclimatization of phytoplankton, to increase photosynthetic rates is to increase the total number of reaction centers. The sensitivity analysis indicates that an increase in the number of photosynthetic units will mostly increase the carbon fixation rates in stratified water, suggesting that the n-strategy would win in this physical scenario. In contrast, Six et al. (2008) suggest the selection of ecotypes with n-strategy in nutrient-rich mixed lagoon waters. It is worth noting that in our model, the cost of the increase of reaction centers is zero, while we can suppose that the cost of building a new reaction center, with its antenna and its electron transport chain, will be high compared with an increase in chlorophyll molecules in an existing antenna (σ-strategy). Our sensitivity analysis also suggests that increase of α^{chl} will favour phytoplankton in low light and stable environments, since it corresponds to the increase in photocapture connected to the σ-strategy (Six et al., 2008). Our results confirm the inadequacy of the σ-strategy for phytoplankton in coastal and mixed waters, where high nutrients concentration may have selected for high-cost n-strategy phytoplankters, and also suggest that

phytoplankton in clear mixed ocean or stable water columns might have high fitness based on the σ-strategy.

Many models so far have focused mostly on photocapture and its modulation in a varying light field. We believe that more effort should be devoted to understanding the role and the cost of photoprotection, not in terms of carbon assimilation but in terms of cell survival, and the regulation of biochemical processes, in response to light variations either in terms of changes in depth, cloudiness, etc. and, more importantly, in terms of circadian variations.

6. Acknowledgements

The authors thanks Dr. Mariella Ragni for helpful discussions on the topic and her and Dr. Fabrizio D'ortenzio for valuable comments on the manuscript, Dr. Euan Brown and Dr. Tim Wyatt for editing the text. The authors also thanks two anonymous referees for constructive criticism of previous versions of this manuscript.

References

T. Anning, H. L. MacIntyre, S. M. Pratt, P. J. Sammes, S. Gibb, and R. J. Geider. Photoacclimation in the marine diatom skeletonema costatum. *Limnol. Oceanogr.*, 45(8):1807–1817, 2000.

M. Baklouti, F. Diaz, C. Pinazo, V. Faure, and B. Queguiner. Investigation of mechanistic formulations depicting phytoplankton dynamics for models of marine pelagic ecosystems and description of a new model. *Prog. Oceanogr.*, 71:1–33, 2006a.

M. Baklouti, V. Faure, L. Pawlowski, and A. Sciandra. Investigation and sensitivity analysis of a mechanistic phytoplankton model implemented in a new modular numerical tool (eco3m) dedicated to biogeochemical modelling. *Prog. Oceanogr.*, 71:34–58, 2006b.

M. J. Behrenfeld, O. Prasil, Z. S. Kolber, M. Babin, and P. G. Falkowski. Compensatory changes in Photosystem II electron turnover rates protect photosynthesis from photoinhibition. *Photosynth. Res.*, 58(3):259–268, 1998.

D. Cianelli, M. Ribera d'Alcala', V. Saggiomo, and E. Zambianchi. Coupling mixing and photophysiological response of antarctic plankton: a lagrangian approach. *Antarct. Sci.*, 16(2):133–142, 2004.

J. J. Cullen and M. R. Lewis. The kinetics of algal photoadaptation in the context of vertical mixing. *J. Plankton Res.*, 10(5):1039–1063, 1988.

K. L. Denman and J. Marra. *Marine Interface Ecohydrodynamics*, chapter Modelling the time dependent photoadaptation of phytoplankton to fluctuating light, pages 341–359. Elsevier, Amsterdam, 1986.

Z. Dubinsky, P. G. Falkowski, and K. Wyman. Light Harvesting and Utilization by Phytoplankton. *Plant Cell Physiol.*, 27(7):1335–1349, 1986.

J. A. Dusenberry. Steady-state single cell model simulations of photoacclimation in a vertically mixed layer: implications for biological tracer studies and primary productivity. *J. Marine Syst.*, 24:201–220, 2000.

P. G. Falkowski and T. G. Owens. Light-shade adaptation two strategies in marine phytoplankton. *Plant Physiol.*, 66:592–595, 1980.

P. G. Falkowski and C. D. Wirick. A simulation model of the effects of vertical mixing on primary productivity. *Mar. Biol.*, 65(1):69–75, 1981.

D. Farmer and C. McNeil. Photoadaptation in a convective layer-Observations. *Deep Sea Res. pt. II*, 46(11):2433–2446, 1999.

K. J. Flynn, H. L. Marshall, and R. J. Geider. A comparison of two N-irradiance interaction models of phytoplankton growth. *Limnol. Oceanogr.*, 46(7):1794–1802, 2001.

P. J. S. Franks and J. Marra. A simple new formulation for phytoplankton photoresponse and an application in a wind-driven mixed-layer model. *Mar. Ecol. Prog. Ser.*, 111(1):143–153, 1994.

E. Garcia-Mendoza, H. C. P. Matthijs, H. Schubert, and L. R. Mur. Non-photochemical quenching of chlorophyll fluorescence in chlorella fusca acclimated to constant and dynamic light conditions. *Photosynth. Res.*, 74(3): 303–315, 2002.

R. J. Geider, H. L. MacIntyre, and T. M. Kana. A dynamic regulatory model of phytoplanktonic acclimation to light, nutrients, and temperature. *Limnol. Oceanogr.*, 43:679–694, 1998.

B. P. Han. A Mechanistic Model of Algal Photoinhibition Induced by Photodamage to Photosystem-II. *J. Theor. Biol.*, 214(4):519–527, 2002.

H. Havelková-Doušová, O. Prášil, and M.J. Behrenfeld. Photoacclimation of Dunaliella tertiolecta (Chlorophyceae) Under Fluctuating Irradiance. *Photosynthetica*, 42(2):273–281, 2004.

J. Huisman, J. Sharples, J. Stroom, P.M. Visser, W.E.A. Kardinaal, J.M.H. Verspagen, and B Sommeijer. Changes in turbulent mixing shift competition for light between phytoplankton species. *Ecology*, 85:2960–2970, 2004.

B. W. Ibelings, B. M. A. Kroon, and L. R. Mur. Acclimation of Photosystem II in a Cyanobacterium and a Eukaryotic Green Alga to High and Fluctuating Photosynthetic Photon Flux Densities, Simulating Light Regimes Induced by Mixing in Lakes. *New Phytol.*, 128(3):407–424, 1994.

D. Kamykowski, H. Yamazaki, and G. S. Janowitz. A lagrangian model of phytoplankton photosynthetic response in the upper mixed layer. *J. Plankton Res.*, 16(8):1059–1069, January 1, 1994 1994.

J. Lavaud, B. Rousseau, H. J. van Gorkom, and A. L. Etienne. Influence of the Diadinoxanthin Pool Size on Photoprotection in the Marine Planktonic Diatom Phaeodactylum tricornutum. *Plant Physiol.*, 129(3):1398–1406, 2002.

H. L. MacIntyre and R. J. Geider. Regulation of rubisco activity and its potential effect on photosynthesis during mixing in a turbid estuary. *Mar. Ecol. Prog. Ser.*, 144:247–264, 1996.

H. L. MacIntyre, T. D. Sharkey, and R. J. Geider. Activation and deactivation of ribulose-1,5-bisphosphate carboxylase/oxygenase (rubisco) in three marine microalgae. *Photosynth. Res.*, 51:93–106, 1997.

H. L. MacIntyre, T. M. Kana, T. Anning, and R. J. Geider. Photoacclimation of photosynthesis irradiance response curves and photosynthetic pigments in microalgae and cyanobacteria. *J. Phycol.*, 38(1):17–38, 2002.

J. Marra. Effect of short-term variations in light intensity on photosynthesis of a marine phytoplankter: A laboratory simulation study. *Mar. Biol.*, 46(3): 191—202, 1978.

C. M. Moore, D. J. Suggett, A. E. Hickman, Y. N. Kim, J. F. Tweddle, J. Sharples, R. J. Geider, and P. M. Holligan. Phytoplankton photoacclimation and photoadaptation in response to environmental gradients in a shelf sea. *Limnol. Oceanogr.*, 51(2):936–949, 2006.

T. Nagai, H. Yamazaki, and D. Kamikowski. A lagrangian photoresponse model coupled with a 2nd-order turbulence closure. *Mar. Ecol. Prog. Ser.*, 265:17–30., 2003.

M. J. Perry, M. C. Talbot, and R. S. Alberte. Photoadaption in marine phytoplankton: Response of the photosynthetic unit. *Mar. Biol.*, 62(2):91–101, 1981.

T. Platt, C.L. Gallegos, and W.G. Harrison. Photoinhibition of photosynthesis in natural assemblages of marine phytoplankton. *Journal of Marine Research*, 38:687–701, 1980.

M. Ragni and M. Ribera d'Alcala'. Circadian variability in the photobiology of phaeodactylum tricornutum: Pigment content. *J. Plankton Res.*, 29(2): 141–156, 2007.

J. A. Raven. Chloroplasts of eukaryotic micro-organisms., 1980.

O. N. Ross, C. M. Moore, D. J. Suggett, H. L. MacIntyre, and R. J. Geider. A model of photosynthesis and photo-protection based on reaction center damage and repair. *Limnol. Oceanogr.*, 53(5):1835–1852, 2008.

E. Sakshaug, A. Bricaud, Y. Dandonneau, P. G. Falkowski, D. A. Kiefer, L. Legendre, A. Morel, J. Parslow, and M. Takahashi. Parameters of photosynthesis: definitions, theory and interpretation of results. *J. Plankton Res.*, 19:1637–1670, 1997.

C. Six, Z.V. Finkel, F. Rodrigez, D. Marie, F. Partensky, and D.A. Campbell. Contrasting photoacclimation costs in ecotypes of the marine eukaryotic picoplankter ostreococcus. *Limnol. Oceanogr.*, 53 (1):255–265, 2008.

M. A. van Leeuwe, B. van Sikkelerus, W. W. C. Gieskes, and J. Stefels. Taxon-specific differences in photoacclimation to fluctuating irradiance in an Antarctic diatom and a green flagellate. *Mar. Ecol. Prog. Ser.*, 288:9–19, 2005.

W. F. Vincent, N. Bertrand, and J. J. Frenette. Photoadaptation to intermittent light across the St. Lawrence Estuary freshwater–saltwater transition zone. *Mar. Ecol. Prog. Ser*, 110:283–292, 1994.

H. Wagner, T. Jakob, and C. Wilhelm. Balancing the energy flow from captured light to biomass under fluctuating light conditions. *New Phytol.*, 169:95–108, 2006.